# Translational regulation contributes to the secretory response of chondrocytic cells following exposure to Interleukin-1β

**Benjamin T McDermott[1], Mandy J Peffers[1], Brian McDonagh[2] and Simon R Tew[1]**

[1] Department of Musculoskeletal Biology, Institute of Ageing and Chronic Disease, University of Liverpool, William Henry Duncan Building, 6 West Derby Street, Liverpool, L7 8TX.
[2] Department of Physiology, School of Medicine, NUI, Galway, Ireland.

Running title: *IL-1β induces translational regulation in chondrocytic cells*

To whom correspondence should be addressed: Benjamin T McDermott: Department of Musculoskeletal Biology, Institute of Ageing and Chronic Disease, University of Liverpool, William Henry Duncan Building, 6 West Derby Street, Liverpool, L7 8TX; benmcd@liverpool.ac.uk; Tel. (0151) 794 9287.

**Keywords:** chondrocyte, inflammation, interleukin 1 (IL-1), osteoarthritis, post-transcriptional regulation, proteomics, superoxide dismutase (SOD).

## ABSTRACT

Osteoarthritis is a chronic disease characterised by the loss of articular cartilage in synovial joints through a process of extracellular matrix destruction that is strongly associated with inflammatory stimuli. Chondrocytes undergo changes to their protein translational capacity during osteoarthritis, but a study of how disease-relevant signals affect chondrocyte protein translation at the transcriptomic level has not previously been performed. In this study we describe how the inflammatory cytokine interleukin 1-beta (IL-1β) rapidly affects protein translation in the chondrocytic cell line SW1353. Using ribosome profiling we demonstrate that IL-1β induced altered translation of inflammatory-associated transcripts such as NFKB1, TNFAIP2, MMP13, CCL2 and CCL7, as well as a number of ribosome-associated transcripts, through differential translation and the use of multiple open reading frames. Proteomic analysis of the cellular layer and the conditioned media of these cells identified changes in a number of the proteins which were differentially translated. Translationally-regulated secreted proteins included a number of chemokines and cytokines, underlining the rapid, translationally-mediated inflammatory cascade that is initiated by IL-1β. Although fewer cellular proteins were found to be regulated in both ribosome profiling and proteomic datasets, we did find increased levels of SOD2, indicative of redox changes within SW1353 cells being modulated at the translational level. In conclusion, we have produced combined ribosome profiling and proteomic datasets which provide a valuable resource in understanding the processes that are occurring during cytokine stimulation of chondrocytic cells.

Osteoarthritis (OA) is a chronic disease characterised by the loss of articular cartilage in synovial joints through a process of extracellular matrix (ECM) destruction, driven by extracellular proteases (1,2). The disease is multifactorial and risk factors include age, genetic predisposition, prior trauma and obesity (3-5). Once considered to be driven primarily by mechanical processes, it is becoming apparent that there is a significant role for inflammation in the pathophysiology of the disease (6,7). The expression of inflammatory cytokines such as interleukin 1-beta (IL-1β) and tumour necrosis factor-alpha (TNF-α) caused by excessive mechanical loading and trauma can contribute to the onset of inflammation and alterations to the articular cartilage due to the promoted actions of catabolic proteases, such as members of the matrix metalloproteinase (MMP) family (8-11). Cytokines are also able to induce catabolic gene expression in chondrocyte cell lines *in vitro*, mimicking many of the processes that occur in chondrocytes during OA development, making them valuable model systems for determining disease mechanisms (12,13). The stable phenotype of a cell line for these *in vitro* studies makes it particularly useful for techniques where large numbers of cells are required, which would be limited by the use of

primary cells. However, when interpreting data from these studies it is important that we focus our interpretation on processes where the cell line best reflects primary cell function.

Changes in the steady state levels of a transcript and its translation rate are not always well correlated (14-17). For some time, studies focussing on specific genes have provided evidence for this and more recently, advances in ribosome footprinting approaches has confirmed this disassociation (18-21). Marker gene expression is often used as a proxy for functional phenotype in disease studies and has led to a significant increase in our understanding of how regulators of disease control the transcriptional landscapes. Although the steady state mRNA levels measured in transcriptomic studies provide important information on the modulation of cellular phenotype under different conditions, they fail to fully inform us about the dynamic post-transcriptional control of mRNA turnover and translation. Such processes represent a vital tier of phenotypic regulation and contribute substantially to the overall functional landscape of the cell.

A number of informative studies have described transcriptomic profiling of cells from healthy and diseased cartilage (22-25), as well as in cell-based models of chondrocyte inflammatory responses (26,27). More recently, our group has demonstrated transcriptome-wide differences in the rates of mRNA decay in chondrocytes from normal and osteoarthritic tissue (24), and have also shown how post-transcriptional regulation via RNA binding proteins affects both anabolic and catabolic gene expression in human chondrocytes (28). These studies coincide with the emerging role for microRNAs in chondrocyte biology, with links between post-transcriptional control of key cartilage degrading proteinases in animal models, human disease and ageing (29-32). Although it is still unclear to what extent discrete control of mRNA translation is involved in the processes that drive OA, there is emerging evidence which suggests that global translation is significantly altered by the disease (33).

Ribosomal profiling is an exciting methodology that utilises RNA sequencing technology to analyse the ribosomal footprints of cellular mRNAs, providing transcriptome-wide resolution of active translation within a cell at a given time. This technique has already led to a number of fresh insights into the mechanisms underlying translation across species, as well as identifying previously unrecognised protein isoforms (34-37). A current requirement for this technique is the relatively large starting quantity of RNA required per sample as only 5-20% of input RNA is recovered after the ribosomal RNA removal step, making analysis of many primary tissue sources extremely challenging. Therefore, in this study we have chosen to use ribosomal profiling and proteomic approaches to examine how translation is altered in an *in vitro* model of chondrocyte response using the SW1353 chondrosarcoma line stimulated with the inflammatory cytokine IL-1β. By examining total mRNA levels, ribosome protected mRNA levels and by performing parallel proteomic analysis, we provide new understanding of how IL-1β regulates genes, as well as identify specific groups of mRNAs where translational and transcriptional level do not necessarily correlate.

## RESULTS

### *Ribosome protected mRNA suitable for RNA-Seq analysis can be isolated from SW1353 cells.*

To determine how IL-1β affected translation rates we performed ribosome profiling analysis on SW1353 cells exposed to the cytokine for 3 hours. Total and ribosome-protected RNA from IL-1β-treated SW1353 cell cultures was isolated and processed for RNA-Seq analysis (Figure 1A; extended workflow shown in Supporting Information Figure S1). Bioanalyser analysis of RNA-Seq libraries showed amplicons with the expected size distributions for each sample (Supporting Information Table S3). Following sequencing, reads were processed and then aligned to the human genome before differential translation analysis was performed using the riboSeqR code via the web-based RiboGalaxy interface. A detailed breakdown of all RiboGalaxy parameters is shown in Supporting Information Table S4. Analysis of triplet periodicity in the ribosomal profiled samples demonstrated that the reads were mostly 28mers with enrichment for those in frame 1, indicating that those reads were in frame with the coded protein. (Figure 1B). Metagene analysis using the plotCDS function confirmed that the 28mer reads were predominantly frame 1 and demonstrated that they were evenly aligned at both the start and end of protein coding regions, with a peak in reads at the translation start site and a small decrease in reads towards the stop codons (Figure 1C).

***Ribosome profiling demonstrates that IL-1β-induced inflammatory secretory proteins in SW1353 cells are differentially translated.***

Differential translation analysis of ribosome protected fragments (RPFs) was performed using the baySeq (38) function via RiboGalaxy and revealed that the majority of the statistically significant ($q<0.001$) top 200 transcripts differentially translated following IL-1β stimulation were increased compared to untreated (Supporting Information Stable S5). Once duplicate transcripts were excluded, there were 112 transcripts for individual proteins. Only four transcripts translated at a lower rate: ZC3H12A, two serine/threonine kinase PIM1 transcripts and one of two transcript variants for TNFAIP2. The majority of the differentially translated transcripts identified as linear mRNA transcripts (93% of transcripts), with the remaining identified as non-coding RNAs or pseudogenes (7% of transcripts; Supporting Information Table S5). STRING analysis of the top 200 differentially translated transcripts identified via ribosome profiling demonstrates that a large proportion coded for either inflammatory-associated proteins (Figure 2A, blue circle; 37 transcripts; 18.5%) or ribosomal-associated proteins (Figure 2A, red circle; 63 transcripts; 31.5%). Interestingly, STRING-derived protein networks from the top 200 statistically significant ($q<0.05$) proteins identified in the secretome data showed similar groupings (Figure 2B). STRING analysis of the 42 proteins significantly differentially regulated ($q<0.05$) in the cellular proteomic analysis identified a cluster of interferon-associated proteins regulated 24 hours after IL-1β stimulation (Figure 2C, grey circle). Commonality between these significantly regulated transcripts/proteins identified by ribosome profiling, cellular proteomic analysis and secretome analysis is illustrated in Figure 2D. A number of proteins that were observed to be differentially translated after 3 hour exposure to IL-1β also exhibited alterations in their absolute level after 24 hours exposure, with examples observed in both the cellular proteome (IFIT2/3 ISG15 and SLC39A14) and in the secretome (CCL2, CCL7, CCL8, , IL6, MMP13, PKM and RPL13,). Taken together, our data suggests that a proportion of the inflammatory response of SW1353 cells to IL-1β treatment occurs as a result of the rapid increase in the translation rates of chemokines, cytokines and associated secretory proteins.

In follow up to this, the levels of CCL2 and IL-6 (both of which showed increased levels of translation and protein secretion in response to IL-1β exposure were measured by ELISA in the media of either SW1353 cells or primary human articular chondrocytes (HACs) exposed to different doses of IL-1β for 24 hours or for different times following stimulation with 10ng/ml IL-1β (Figure 3). Interestingly, the primary cells were more responsive to lower doses of IL-1β. This was particularly striking in the CCL2 data where the lowest concentration of IL-1β (0.1ng/ml, Figure 3B) was able to elicit a significant increase in CCL2 secretion, whereas SW1353 secretion only increased at 5ng/ml and above (Figure 3A). A similar result was found for the IL-6 data (Figure 3E and F), although variance of donor response for the primary chondrocytes precludes statistical confirmation of this with the current sample size. For both CCL2 and IL6, the SW1353 cells (Figure 3C and G) and the primary chondrocytes (Figure D and H) exhibited similar longitudinal secretory responses to 10ng/ml IL-1β, the experimental concentration used in Ribo-Seq and proteomic parts of the study.

***IL-1β induces altered translation of inflammatory-associated transcripts and translation via multiple open reading frames.***

We examined Ribo-Seq and total RNA-Seq reads for differentially translated genes. Reads from each reading frame (measured against left hand y-axis) were plotted on top of total RNA-Sequencing reads (plotted against right hand y-axis) using the RiboGalaxy platform (Figure 4). The x-axis of these charts represents the entire length of the particular transcript with the coding domain sequence indicated. Some of the differentially translated transcripts examined, e.g. NKFB1 (Figure 4A) and TNFAIP2 (Figure 4B), exhibited an increase in both the total RNA counts and ribo-counts, suggesting and increase in both transcription and translation. Interestingly, some of the differentially translated transcripts exhibited a marked reduction in total RNA reads whilst simultaneously showing an increase in RPF reads, indicating reduced transcription rates and/or increased rates of turnover alongside an increased rate of translation. Examples of this were found for the chemokines CCL2 and CCL7 (Figure 4C and D) and the NFkB signalling component

NFKB1Z (Figure 4E). We also observed clustered ribosome protected reads outside of the normal transcript protein coding sequence (CDS), within discrete regions of the 3'UTR, for a limited set of genes. Examples of these were reads observed in the 3'UTR for TNFAIP2 (Figure 4B) and for SOX9 (Figure 4F) (although note that SOX9 was only in the top 200 of differentially translated transcripts when all three reading frames were examined together and not when focusing on frame 1 from the triplet periodicity data). For SOX9, the increase in ribo-counts came mostly from regions within the SOX9 3'UTR, suggesting that translation of SOX9 was not increased but instead, there was an increase in ribosome occupation or interaction at this region in response to IL-1β stimulation.

Despite the triplet periodicity and metagene analysis of 28mer RPFs showing that the majority of transcripts were from protein coding regions within frame 1 (Figure 1B and 1C), individual riboplots for some transcripts that were identified as being differentially translated show that transcripts were being translated from more than one open reading frame (ORF). For example, the riboplot for CCL2 (Figure 4C) shows that after IL-1β treatment there was an increase in CCL2 ribo-counts in frame 2 and frame 3. Whereas for CCL7 (Figure 4D), the majority of ribo-counts increased after IL-1β treatment were from frame 1, with just a couple from frames 2 and 3. Taken together, these results suggest that while the number of mRNA transcripts may increase or decrease in response to IL-1β treatment, rates of active mRNA translation do not necessarily reflect changes in transcription.

***IL-1β induces redox changes in SW1353 cells.***

Results from the SW1353 cellular proteomic data showed that SOD2 was one of the highest ranked, differentially expressed proteins following exposure to IL-1β (Supporting Information Table S1). When ribosome profiling data from all three frames was analysed, SOD2 was identified as one of the most highly differentially translated transcripts The riboplot for SOD2 (Figure 5A) showed that SOD2 reads were predominantly in frame 3 and of all the transcripts examined, show the largest increase in ribo-counts following IL-1β treatment (from 55 to 1509). Total RNA read coverage for SOD2 remained largely unchanged however, strongly suggesting that IL-1β significantly increases SOD2 levels at the translational level. Western blotting of cellular lysates from IL-1β (10 ng/ml) treated SW1353 showed that this increase in translation also resulted in an increase in protein expression in a time-dependent manner when (Figure 5B, left panel). After 24 hours of IL-1β stimulation at a range of IL-1β concentrations, SOD2 levels were also increased (Figure 5B, right panel). However, it is currently unknown at what timeframe this SOD2 expression took place.

To further investigate the possibility that IL-1β treatment causes redox changes, ROS detection assays were carried out. Results show that with 10 ng/ml IL-1β treatment, there is a significant level of variance of ROS activity over time (Figure 5C, left panel). IL-1β treatment appears to quickly induce levels of ROS, which then reduce with time in correlation to SOD2 protein expression via western blotting (left panels of Figures 5B and C). Concentrations of IL-1β as low as 0.1ng/ml resulted in an increase in ROS activity (Figure 5C, right panel) but still induced SOD2 at similar levels to 10 ng/ml dose after 24 hours. This data, along with the increase in NFKB1 mRNA expression and translation (Figure 4A) suggest that IL-1β treatment activates NFκB and a cellular stress response within the SW1353 cells, which is controlled through translational mechanisms.

**DISCUSSION**

In order to study how IL-1β alters translation using ribosome profiling, a suitable model system was required which maintained biologically relevant aspects of cell function with the practical requirements of obtaining relatively large quantities of total RNA. The number of cells required for ribosome profiling made the use of freshly isolated primary chondrocytes unfeasible, whilst expansion of these cells results in a progressive loss of phenotype that quickly leads to them sharing the majority of their transcriptomic signature with cultured cells from connective tissues such as tendon (39). We were therefore attracted to the use of a chondrocytic cell line that exhibited similar responsiveness to IL-1β as primary chondrocytes. Gebauer *et al*. (13) found that the SW1353 chondrosarcoma cell line displayed considerably reduced expression of ECM components, but were still a valuable system for investigating catabolic gene regulation by IL-1β. In line with this, our data has shown there is an increase in IL-1β, IL-6, LIF, NFKB1 and TNFAIP6 mRNA expression following IL-1β stimulation (Supporting Information Table S5)

which replicates that observed in IL-1β-treated HAC by Gebauer *et al*. (13). There are always limitations to accept with such cell lines, of course and there is evidence that SW1353 and another chondrocyte cell line, T/C-28a2, do not regulate inducible nitric oxide synthase expression in the same way as HACs following stimulation with pro-inflammatory cytokines (40). However, in this instance, we decided to use the SW1353 cell line as an *in vitro* replacement for HACs.

We believe that this is the first time that ribosome profiling has been used to study a chondrocytic cell type. Ribosome protected fragments were detected from 26 – 30 nucleotides in length, with the majority being 28mers (Figure 1B). Metagene analysis with our ribosome profiling data showed that most RPFs were found relatively evenly across protein coding regions, as expected. However, there were instances where RPFs were found within the 3'UTR, such as in TNFAIP2 (Figure 4B) and SOX9 (Figure 4F). Miettinen and Bjorklund (41) suggest that this association of ribosomes with the 3'UTR could be due to migration of the ribosome through the stop codon, or the 3'UTR folding round on itself and associating with ribosomes on the CDS. Therefore, the potential for interactions with ribosomes and the 3'UTR of these mRNAs suggest a role in translational regulation. Given the well-established role of these two proteins in cartilage biology, this may represent an interesting new regulatory mechanism controlling cartilage function.

Whilst it appears from our complementary proteomic and ribosome profiling data that IL-1β treatment results in an up-regulation of ribosomal-associated transcripts and transcripts for inflammatory mediators, the presence of ribosomal-associated proteins in the SW1353 secretome at first seemed unusual. However, the source of ribosomal-associated proteins in the media samples could be due to the presence of exosomes, which are constantly secreted by all cells in culture. Exosomes are small vesicles (30-150 nm) containing up to thousands of proteins and small RNAs and they have a variety of functions such as facilitation of the immune response, antigen presentation, programmed cell death and inflammation (42). Exosomes are also a novel mechanism for cell-to-cell communication (43). Another possibility for the source of ribosomal-associated proteins in the cell culture media is due to cell lysis at the point of media harvesting and the presence of Actin and other Actin-related proteins (Supporting Information Table S2) supports this theory. There was also a large proportion of ribosomal-associated transcripts identified through ribosome profiling differential translation analysis. It is not clear whether this change is a specific response to IL-1β or a general response induced by a potential alteration in the translational burden on the cells during their response.

Differential translation analysis in this study showed that as well as ribosomal-associated and inflammatory mediator-associated transcripts being up-regulated in response to IL-1β treatment, the expression of 14 pseudogenes, 9 of which were pseudogenes for ribosomal proteins, were also detected. Ribosomal protein pseudogenes represent the largest class of pseudogenes within the human genome (44) and ribosomal pseudogenes have been detected in many human tissues, but their function remains unclear (45). Differential translation analysis also found that IL-1β treatment decreased the translation of only two transcripts; PIM1 and ZC3H12A. PIM1 is a proto-oncogene with serine/threonine kinase activity involved in cell survival, proliferation and apoptosis (46). As exogenous IL-1β treatment has been shown to both stimulate and inhibit apoptosis in different cell systems (47), the decrease in PIM1 expression seen here could suggest that IL-1β treatment could be activating apoptosis in this system, although no other apoptotic-associated transcripts were detected in the differential translation analysis. ZC3H12A is a transcriptional activator with endoribonuclease activity that is involved in a variety of biological functions, including the cellular inflammatory response. IL-1β has been shown to up-regulate ZC3H12A expression via the NFκB and ERK pathways (48), which is contrary to what was found in this study.

The riboplots in Figure 4 show that some transcripts, such as NFKB1 and TNFAIP2 experience an increase in transcript level and translation rate following IL-1β exposure, whereas other transcripts such as CCL2, CCL7, and NFKB1Z experience a simultaneous reduction in transcript level with an increase in translation. This observation of genes under both transcriptional and translational control has also been observed by others (49,50) and confirms the complexity of gene regulation. Elevation of CCL2 and CCL7 in particular represent a primed, early response to IL-1β stimulation which is likely to be characterised by rapid secretion that

will be quickly switched off. The role of the rapid, translationally mediated secretion of chemokines by chondrocytes may represent an important, physiological means of cell to cell signalling in healthy tissue and merits further study.

OA was once considered to be a non-inflammatory disease, caused by excessive wear and tear on the articular cartilage of the affected joint. More recently however, it has been recognised that inflammation plays a significant role in OA pathogenesis (7,8,51). In both diseased tissue and in this *in vitro* model, the onset of inflammation by inflammatory cytokines such as IL-1β, up-regulates the expression of transcripts that code for enzymes such as MMP13, which causes further cartilage degradation (52). Reactive oxygen species (ROS) and oxidative stress have also been shown to play a significant role in OA progression (53,54) and through the activation of the redox-sensitive NFκB transcription factor, chondrocytes increase SOD2 production to prevent ROS-mediated damage (55-57). Across the three areas studied here, cellular proteome, secretome and translatome, activation of NFκB in response to IL-1β was consistent. The increase in SOD2 translation and protein expression in this SW1353 model suggests IL-1β induces changes in the mitochondrial redox balance through translational regulation. ROS levels rise rapidly upon IL-1β stimulation and drop as production of SOD2 rises. However, low levels of IL-1β (e.g.01.ng/ml) can lead to increased ROS generation at 24-hours despite SOD2 levels increasing, suggesting that there is a greater complexity to the mechanism of cytokine responsive redox control in these cells.

The mechanisms through which chondrocyte translation is regulated has not been thoroughly studied. However, two pioneering recent recent studies has shown that osteoarthritic and cytokine mediated translational changes in chondrocytes are mediated by the activity of the CAP dependent translation repressor 4E binding protein 1 (58), possibly acting downstream of mechanistic target of rapamycin complex 1 signalling (59). In addition, small RNAs that are known to regulate translation, such as microRNAs and snoRNAs are known to differentially expressed in normal and osteoarthritic cartilage (60,61). The influences of these mechanisms on the translation of many of the transcripts identified in this study is clearly now warranted.

In summary, this study shows for the first time the use of ribosome profiling in a chondrocytic cell, observing the effects of IL-1β on translational regulation. We have shown that through differential translation IL-1β can induce the secretion of inflammatory proteins and promote changes in redox regulators in these cells. It is possible that chondrocytes are primed to rapidly respond to inflammatory cytokine stimulation, producing a cascade of further inflammatory mediators. Whether there is a role for this rapid responsiveness in the maintenance tissue homeostasis in healthy tissue remains, for now, a key unanswered question.

## EXPERIMENTAL PROCEDURES

### *Cell culture*

The SW1353 chondrosarcoma cell line (ATCC HTB-94) was cultured in Dulbecco's Modified Eagles Medium (DMEM, ThermoFisher Scientific, 31885023) containing 10% Foetal Bovine Serum (FBS, Sigma, F7524), 100 units/ml penicillin-streptomycin (Gibco, 15140122) and 5 µg /ml amphotericin B (Gibco, 15290018), cultured at 37 °C in a 5% $CO_2$ environment. Osteoarthritic human articular cartilage (HAC) was obtained with approval from the Cheshire Research Ethics Committee following total knee arthroplasty. Primary articular chondrocytes were isolated from cartilage tissue using the medium described above, supplemented with 0.08% type II collagenase (Worthington Biochemical), overnight at 37 °C. Cells were cultured as described for SW1353.

### *Proteomic mass spectrometry and label-free quantification*

To determine how protein secretion and cellular proteome changes were affected by cytokine stimulation, SW1353 cells were cultured for 24 hours in the presence or absence of 10 ng/ml IL-1β in serum-free, phenol red-free DMEM (n=3 for each condition). Media was collected from the cells and then subjected to in-solution trypsin digestion and LC-MS/ MS (see below). Protein extracts from the SW135 cell layer were prepared were prepared in 50mM ammonium bicarbonate containing 25 mM N-ethylmaleimide (d(0) NEM) pH 8. Protein lysates were prepared by centrifugation at 15,000 x*g* for 10min at 4 °C. Excess d(0) NEM was removed using Zeba desalting columns (ThermoFisher Scientific) and protein concentrations were determined using Bradford

assay (BioRad) with BSA as a standard. 100 µg of protein extract was diluted to 160 µl with 25 mM ammonium bicarbonate and denatured by the addition of 10 µl of 1% RapiGest (Waters, Manchester, UK) in 25 mM ammonium bicarbonate and incubated at 80 °C for 10 min with shaking. 10 µl of a 100 mM solution of Tris(2-carboxyethyl)phosphine hydrochloride (TCEP) was added to reduce reversibly oxidised Cys residues followed by incubation at 60 °C for 10 min. Newly reduced Cys were then alkylated by addition of d(5) NEM and incubated at room temperature for 30 min. An aliquot of the samples was used at this point to check procedure by SDS-PAGE. Proteolytic digestion was performed by addition of trypsin followed by overnight incubation at 37 °C. Digestion was terminated and RapiGest removed by acidification (3 µl of TFA and incubated at 37 °C for 45min) and centrifugation (15,000 x*g* for 15 min).

Mass spectrometry was performed using an Ultimate 3000 RSLC™ Nano system (ThermoFisher Scientific) coupled to a QExactive™ mass spectrometer (ThermoFisher Scientific). 250 ng per sample were loaded onto the trapping column (Thermo Scientific, PepMap100, C18, 75 µm X 20 mm), using partial loop injection, for seven minutes at a flow rate of 4 µL/min with 0.1% (v/v) TFA. The sample was resolved on the analytical column (Easy-Spray C18 75 µm x 500 mm 2 µm column) using a gradient of 97% A (0.1% formic acid) 3% B (99.9% ACN 0. 1% formic acid) to 60% A 40% B over 120 minutes at a flow rate of 300 nL/min. The program used for data acquisition consisted of a 70,000 resolution full-scan MS scan (AGC set to 106 ions with a maximum fill time of 250 ms) the 10 most abundant peaks were selected for MS/MS using a 17,000 resolution scan (AGC set to 5 X 104 ions with a maximum fill time of 250 ms) with an ion selection window of 3 m/z and a normalized collision energy of 30. To avoid repeated selection of peptides for MS/MS the program used a 30 second dynamic exclusion window.

Label-free relative quantification software PEAKS™ 7 (Bioinformatics Solutions Inc, Waterloo, Canada) was used to analyse RAW data files against the same mouse protein database for identifications with Mascot. Proteins were considered significantly changed between 0 and 24 hour IL-1β-treated samples using a -10logP score > 20 (equivalent to a P value < 0.01), a fold change > 2 and at least 3 unique peptides. The full list of identified proteins including statistical analysis is included in Supporting Information Table S1.

Protein concentrations of media samples from SW1353 cultured for 24 hours in the presence or absence of 10 ng/ml IL-1β in serum-free, phenol red-free DMEM (n=3 for each condition), were estimated by Bradford assay using Coomassie Plus™ protein assay reagent (ThermoFisher Scientific, 23236) read at 600nm. Prior to trypsin digestion, the protein concentration of each sample was calculated using the Pierce™ 660 nm protein assay (ThermoFisher Scientific, 22662). In-solution tryptic digest was carried out on 10 µl of StrataClean resins (Agilent Genomics, 400714) on 100 µg protein for each sample as previously described (62). LC-MS/MS was performed using an Ultimate 3000 RSLC™ Nano system (ThermoFisher Scientific) coupled to a QExactive™ mass spectrometer (ThermoFisher Scientific). Tryptic peptides (250 ng) from randomised samples were loaded onto the column on a 2 hour gradient with an inter-sample 30 min blank (63).

***Western blotting***

For western blotting homogenised protein lysates were diluted using laemmli buffer and 20 µg of protein separated on 12 % SDS-PAGE gels. Proteins were transferred using a semi-dry blotter. Membranes were blocked in Odyssey blocking buffer in TBS (Licor, 927-50000) and then incubated with primary antibody for SOD2 (Cell Signaling Technology, 13194) at a dilution of 1:750 in blocking buffer. IRDye 800CW Goat anti-rabbit secondary antibody (Licor, 925-32210) was diluted 1:10,000 in blocking buffer. Antibody signal was detected using the Odyssey CLx imaging system (Licor) and images were acquired and analysed usingthe Image Studio Acquisition software (Licor). Total protein staining was carried out using InstantBlue Protein Gel Stain (Expedeon, ISB1L), then imaged using the ChemiDoc XBS+ Molecular Imager (BioRad) and Image Lab software (BioRad).

***CCL2 and IL-6 ELISAs***

SW1353 and HACs were treated with 0, 0.1, 0.5, 1, 5 and 10 ng/ml IL-1β for 24 hours, or with 10 ng/ml IL-1β for 0, 1, 3, 6, 24 and 48 hours and medium was harvested for CCL2 (R&D Systems, DY279) and IL-6 (R&D

Systems, DY206) ELISAs. For IL-1β concentration-dependent treatment, HAC donors M70, M76 and M86 were used. For time dependent IL-1β treatment, HAC donors M69, F80 and F86 were used. Optical density was measured using the SPECTROstar Nano spectrophotometer (BMG Labtech) and the MARS data analysis software (BMG Labtech). Cytokine secretion levels were normalised to either 0 ng/ml IL-1β, or 0h treatment. Charts were plotted and statistical analysis (ANOVA and Dunnett's multiple comparison test) was performed using Prism (GraphPad). Data was considered statistically significant if P-value was <0.05.

***ROS detection assay***

For ROS detection, SW1353 were treated with IL-1β (ranging from 0 to 10 ng/ml) for 24 hours, or with 10 ng/ml IL-1β for 0, 0.5, 1, 3, 6, 24, 30 and 48 hours in 96-well plates. $H_2O_2$ treatment (200 μm for 2 hours) served as a positive control for ROS production. ROS detection was carried out using CM-$H_2$DCFDA (ThermoFisher Scientific, C6827). Fluorescence was measured using the SPECTROstar Nano spectrophotometer (BMG Labtech) and the MARS data analysis software (BMG Labtech). Charts were plotted and statistical analysis (Dunnett's multiple comparison test) was performed using Prism (GraphPad). Data was considered statistically significant if P-value was <0.05.

***Purifying ribosome protected RNA***

Ribosome profiling was carried out similar to the method described by Ingolia *et al*. (64), modified with the use of the ARTseq (Mammalian) Ribosome Profiling Kit (Epicentre, RPHMR12126). Serum was withdrawn when the cells had reached ~80% confluence and then 24 hours later the cells were treated with 10 ng/ml IL-1β (Sigma, I9401) for 3 and 24 hours (3x 175cm$^2$ flasks per time point, n=3).

To harvest cells for ribosome profiling, cell culture media was removed and cells were washed with ice-cold PBS containing 0.1 mg/ml cycloheximide (Millipore UK Ltd, 239763). Cells were scraped into 800 μl mammalian lysis buffer (20% v/v 5x Mammalian Polysome Buffer (supplied in ARTseq RP Kit), 1% v/v Triton X-100 (supplied), 10 mM DTT (supplied), 10 U/μl DNase I (supplied), 0.1 mg/ml cycloheximide), then passed through a 22-25 G needle to lyse the cells completely. Cell lysate was then incubated on ice for 10 minutes and then centrifuged for 10 minutes at 20,000 x*g* at 4 °C. The supernatant was transferred to a pre-chilled tube and kept on ice. A 1:10 dilution of the clarified supernatant was prepared using nuclease-free water and the $A_{260}$ reading of the lysate was determined using a nanodrop spectrophotometer. For each sample, the supernatant was split into 100 μl aliquots and to one aliquot, 10 μl 10% SDS was added and served as the 'Total RNA' sample. To the remaining 100 μl aliquots, 5 units of ARTseq Nuclease was added for each $A_{260}$ of lysate and incubated at room temperature for 45 minutes with gentle mixing. Nuclease digest reactions were stopped by the addition of 300 U of SUPERase•In Inhibitor (ThermoFisher Scientific, AM2696). The ribosome protected fragments (RPFs) were purified according to the ARTseq Ribosome Profiling Kit (Mammalian) protocol. Briefly, the 100 μl aliquots that were nuclease digested earlier were added to Micro-Spin S-400 columns (GE Healthcare, 27-5140-01), which had been equilibrated by gravity flow with 3 ml of 1x Mammalian Polysome Buffer and centrifuged for two minutes at 600 x*g*. The flow-through was collected and 10 μl 10% SDS was added – this then served as the 'Ribosome Protected RNA' (RPF) sample.

***RNA purification and ribosome depletion***

Total and RPF RNA samples were purified using the TRIzol/chloroform method. Ribosomal RNA (rRNA) was depleted from the Total and RPF RNA samples using the Ribo-Zero rRNA Removal Kit (Epicentre, RHZ110424). Briefly, 1-5 μg of RNA was incubated at 68 °C for 10 minutes with Ribo-Zero rRNA Removal Solution (supplied) and then at room temperature for 15 minutes, before mixing with pre-prepared microspheres (supplied). Hybridised RNA-microspheres were incubated at room temperature with frequent mixing for 10 minutes to allow rRNA to bind to the microspheres, which were then removed by centrifuging the sample at 12,000 x*g* in a Microsphere Removal Unit (supplied). The filtrate containing the rRNA-depleted RNA was then purified using the TRIzol/chloroform protocol described above. rRNA-depleted Total RNA samples were then heat fragmented (see below) and RPF RNA samples were then PAGE purified.

***Fragment and end repair and 3'Adaptor ligation***

rRNA-depleted Total RNA samples were heat fragmented at 94 °C for 20 minutes and then held at 4 °C. Both heat fragmented Total RNA samples and PAGE purified RPF RNA samples were then end repaired using ARTseq PNK enzyme, incubating for 1 hour at 37 °C. RNA samples were then purified using the TRIzol/chloroform protocol and eluted into 10 µl nuclease-free water. RNA samples were incubated with the supplied ARTseq 3'Adaptor (supplied) for 2 minutes at 65 °C and then held at 4 °C. These denatured RNA samples were then incubated with the supplied ARTseq Ligase (supplied), ligation buffer (supplied) and 100 mM DTT at 23 °C for 2 hours. The supplied ARTseq AR Enzyme (supplied) was then added to this ligation mix and incubated at 30 °C for 30 minutes. RNA samples were then reverse transcribed.

***cDNA synthesis and circularisation***

The 3'adaptor-ligated RNA samples were reverse transcribed using the supplied EpiScript Reverse Transcriptase (supplied) at 50 °C for 30 minutes. Reverse transcription samples were then incubated with the supplied ARTseq Exonuclease (supplied) at 37 °C for 30 minutes and then 80 °C for 15 minutes before adding the ARTseq RNase mix (supplied) and incubating the samples at 55 °C for 5 minutes. Samples were then held at 4 °C before PAGE purifying the cDNAs on 10% polyacrylamide/7-8M urea/TBE gels using bromophenol blue at 180 V with SYBR Gold (ThermoFisher Scientific, S11494) staining. cDNA was circularised using the supplied CircLigase (supplied) by incubating for 2 hours at 60 °C with the ARTseq CircLigase Reaction Mix (supplied), ATP and $MnCl_2$ (both supplied), before holding at 4 °C. Circularised cDNA was then PCR amplified as described below.

***PCR amplification***

Circularised cDNA (5 µl) was mixed with 2 µl of the ARTseq Forward PCR Primer (supplied), 2 µl of a ScriptMiner Index PCR primer of choice (supplied index primers 1-12) and 25 µl 2x Phusion High-fidelity PCR Master Mix (New England Biolabs, M0531) in a total volume of 50 µl. Samples were then ran in following PCR program: 98 °C for 30 seconds, then 15 cycles of 94 °C for 15 seconds, 55 °C for 5 seconds and 65 °C for 10 seconds. PCR products were purified using the Agencourt AMPure XP beads (Beckman Coulter, A63880) according to the manufacturer's instructions and eluted into 25 µl nuclease-free water. To check for successful PCR amplification, 2.5 µl of the PCR amplified samples was mixed with 6x native gel loading dye and run on a Novex 8% NativeTBE gel (Thermo Fisher Scientific, EC6215BOX) at 200 V until the dye front reached the bottom of the gel, with ΦX174 RF DNA/HAE III fragments as markers (ThermoFisher Scientific, 15611-015). The gel was then stained with SYBR Gold and visualised using a dark field transilluminator. Samples that contained successfully amplified libraries (140-160 bp) were sent for QC and sequencing.

***Quality control and sequencing***

Successfully amplified PCR libraries were sent to the University of Liverpool's Centre for Genomic Research for sequencing. Samples were quantified using a Qubit dsDNA High Sensitivity Kit (Life Technologies, Q32854) and a Bioanalyser DNA High Sensitivity Kit (Agilent, 5067-4626), using 1 µl per sample of a 2 ng/µl dilution of each library. Libraries were then pooled at equi-molar quantities and the pooled libraries were size selected within 120-160 bp on a SAGE PippinPrep instrument using a 1.5% agarose gel cassette. The size selected pooled library was assessed by Bioanalyser and subsequently by qPCR using the Illumina Library Quantification Kit (KAPA Biosystems, KK4854) on a Roche Light Cycler LC480II according to the manufacturer's instructions. The template DNA was denatured according to the protocol described in the Illumina cBot User Guide and loaded a at 12 pM concentration. Sequencing was performed using an Illumina HiSeq2500 with 125 bp reads at the Centre for Genome Research at the University of Liverpool. A summary of the quality control data can be found in supporting information Table S3.

***RNA-Seq data analysis***

The total number of reads from each sample varied from 7.5 $x10^6$ to 5.9 $x10^7$. FASTQ files containing reads from ribosome protected and total RNA sample were uploaded to the RiboGalaxy server where sequences were first trimmed to remove adapter sequences. Following this ribosomal RNA reads were removed from the data and then riboSeqR was used via the RiboGalaxy interface to align

remaining reads to the human genome (GRCh38) before performing differential translation analysis (65). A detailed description of the workflow and RiboGalaxy parameters can be found in Supporting Information Figure S1 and Table S4, respectively.

***Functional gene characterisation and protein networks.***

Ribosome profiling and proteomic data was submitted to the Database for Annotation, Visualisation and Integrated Discovery (DAVID) online analysis program (Version 6.8, https://david.ncifcrf.gov/). Functional and physical interactions between proteins were discovered using the online STRING Protein-Protein Interaction Network (https://string-db.org/)

***Data deposition***

The RNA-seq data representing both total and ribosome-protected RNA have been deposited in ArrayExpress (accession number E-MTAB-7466). Both cellular proteomic and secretome data have been deposited in PRIDE (accession number PXD012985).

**Acknowledgements:** We would like to thank Pia Koldkjær from the Centre for Genome Research at the University of Liverpool for performing the Illumina HiSeq2500 sequencing, as well as James Mullan and Audry Michel for assistance with the RiboGalaxy platform. This work was supported by Biotechnology and Biological Sciences Research Council grant BB/K00381X/1, Medical Research Council grant MR/N011333/1 and the University of Liverpool Technology Directorate.

**Conflict of interest:** The authors declare that they have no conflicts of interest with the contents of this article.

**Author contributions:** BTM, MJP and SRT designed the experiments. BTM performed the ribosome profiling and analysed the corresponding results. MJP performed culture media secretome analysis. BM performed cellular proteomic analysis. BTM and SRT wrote the manuscript.

**REFERENCES**


1. Troeberg, L., and Nagase, H. (2012) Proteases involved in cartilage matrix degradation in osteoarthritis. *Biochimica et Biophysica Acta (BBA) - Proteins and Proteomics* **1824**, 133-145
2. Verma, P., and Dalal, K. (2011) ADAMTS-4 and ADAMTS-5: Key enzymes in osteoarthritis. *Journal of Cellular Biochemistry* **112**, 3507-3514
3. Cooper, C., Snow, S., McAlindon, T. E., Kellingray, S., Stuart, B., Coggon, D., and Dieppe, P. A. (2000) Risk factors for the incidence and progression of radiographic knee osteoarthritis. *Arthritis & Rheumatism* **43**, 995-1000
4. Silverwood, V., Blagojevic-Bucknall, M., Jinks, C., Jordan, J. L., Protheroe, J., and Jordan, K. P. (2015) Current evidence on risk factors for knee osteoarthritis in older adults: a systematic review and meta-analysis. *Osteoarthritis and Cartilage* **23**, 507-515
5. Spector, T. D., and MacGregor, A. J. (2004) Risk factors for osteoarthritis: genetics11Supported by Procter & Gamble Pharmaceuticals, Mason, OH. *Osteoarthritis and Cartilage* **12**, 39-44
6. Greene, M. A., and Loeser, R. F. (2015) Aging-related inflammation in osteoarthritis. *Osteoarthritis and Cartilage* **23**, 1966-1971
7. Sokolove, J., and Lepus, C. M. (2013) Role of inflammation in the pathogenesis of osteoarthritis: latest findings and interpretations. *Therapeutic Advances in Musculoskeletal Disease* **5**, 77-94
8. Goldring, M. B., and Otero, M. (2011) Inflammation in osteoarthritis. *Current opinion in rheumatology* **23**, 471-478
9. Shi, J., Schmitt-Talbot, E., DiMattia, D. A., and Dullea, R. G. (2004) The differential effects of IL-1 and TNF-α on proinflammatory cytokine and matrix metalloproteinase expression in human chondrosarcoma cells. *Inflammation Research* **53**, 377-389
10. Stone, A. V., Loeser, R. F., Vanderman, K. S., Long, D. L., Clark, S. C., and Ferguson, C. M. (2014) Pro-inflammatory stimulation of meniscus cells increases production of matrix metalloproteinases and additional catabolic factors involved in osteoarthritis pathogenesis. *Osteoarthritis and cartilage / OARS, Osteoarthritis Research Society* **22**, 264-274
11. Wojdasiewicz, P., Poniatowski, L., and Szukiewicz, D. (2014) The Role of Inflammatory and Anti-Inflammatory Cytokines in the Pathogenesis of Osteoarthritis. *Mediators of Inflammation* **2014**, 19
12. Barksby, H. E., Hui, W., Wappler, I., Peters, H. H., Milner, J. M., Richards, C. D., Cawston, T. E., and Rowan, A. D. (2006) Interleukin-1 in combination with oncostatin M up-regulates multiple genes in chondrocytes: Implications for cartilage destruction and repair. *Arthritis & Rheumatism* **54**, 540-550
13. Gebauer, M., Saas, J., Sohler, F., Haag, J., Söder, S., Pieper, M., Bartnik, E., Beninga, J., Zimmer, R., and Aigner, T. (2005) Comparison of the chondrosarcoma cell line SW1353 with primary human adult articular chondrocytes with regard to their gene expression profile and reactivity to IL-1β. *Osteoarthritis and Cartilage* **13**, 697-708
14. Abreu, R. d. S., Penalva, L. O., Marcotte, E. M., and Vogel, C. (2009) Global signatures of protein and mRNA expression levels. *Molecular bioSystems* **5**, 1512-1526
15. Greenbaum, D., Colangelo, C., Williams, K., and Gerstein, M. (2003) Comparing protein abundance and mRNA expression levels on a genomic scale. *Genome Biology* **4**, 117
16. Larsson, O., Sonenberg, N., and Nadon, R. (2010) Identification of differential translation in genome wide studies. *Proceedings of the National Academy of Sciences of the United States of America* **107**, 21487-21492
17. Maier, T., Güell, M., and Serrano, L. (2009) Correlation of mRNA and protein in complex biological samples. *FEBS Letters* **583**, 3966-3973
18. Ingolia, N. T., Lareau, L. F., and Weissman, J. S. (2011) Ribosome Profiling of Mouse Embryonic Stem Cells Reveals the Complexity of Mammalian Proteomes. *Cell* **147**, 789-802
19. Michel, A. M., and Baranov, P. V. (2013) Ribosome profiling: a Hi-Def monitor for protein synthesis at the genome-wide scale. *Wiley Interdisciplinary Reviews. RNA* **4**, 473-490
20. Pop, C., Rouskin, S., Ingolia, N. T., Han, L., Phizicky, E. M., Weissman, J. S., and Koller, D. (2014) Causal signals between codon bias, mRNA structure, and the efficiency of translation and elongation. *Molecular Systems Biology* **10**, 770

21. Xiao, Z., Zou, Q., Liu, Y., and Yang, X. (2016) Genome-wide assessment of differential translations with ribosome profiling data. *Nature Communications* **7**, 11194
22. Aigner, T., Saas, J., Zien, A., Zimmer, R., Gebhard, P. M., and Knorr, T. (2004) Analysis of Differential Gene Expression in Healthy and Osteoarthritic Cartilage and Isolated Chondrocytes by Microarray Analysis. *Cartilage and Osteoarthritis. Methods in Molecular Medicine* **100**, 109-127
23. Sato, T., Konomi, K., Yamasaki, S., Aratani, S., Tsuchimochi, K., Yokouchi, M., Masuko-Hongo, K., Yagishita, N., Nakamura, H., Komiya, S., Beppu, M., Aoki, H., Nishioka, K., and Nakajima, T. (2006) Comparative analysis of gene expression profiles in intact and damaged regions of human osteoarthritic cartilage. *Arthritis & Rheumatism* **54**, 808-817
24. Tew, S. R., McDermott, B. T., Fentem, R. B., Peffers, M. J., and Clegg, P. D. (2014) Transcriptome-Wide Analysis of Messenger RNA Decay in Normal and Osteoarthritic Human Articular Chondrocytes. *Arthritis & Rheumatology (Hoboken, N.j.)* **66**, 3052-3061
25. Peffers, M. J., Liu, X., and Clegg, P. D. (2014) Transcriptomic profiling of cartilage ageing. *Genomics Data* **2**, 27-28
26. Sandell, L. J., Xing, X., Franz, C., Davies, S., Chang, L.-W., and Patra, D. (2008) EXUBERANT EXPRESSION OF CHEMOKINE GENES BY ADULT HUMAN ARTICULAR CHONDROCYTES IN RESPONSE TO IL-1β. *Osteoarthritis and cartilage / OARS, Osteoarthritis Research Society* **16**, 1560-1571
27. Vincenti, M. P., and Brinckerhoff, C. E. (2001) Early response genes induced in chondrocytes stimulated with the inflammatory cytokine interleukin-1beta. *Arthritis Research* **3**, 381-388
28. McDermott, B. T., Ellis, S., Bou-Gharios, G., Clegg, P. D., and Tew, S. R. (2016) RNA binding proteins regulate anabolic and catabolic gene expression in chondrocytes. *Osteoarthritis and Cartilage* **24**, 1263-1273
29. Balaskas, P., Goljanek-Whysall, K., Clegg, P., Fang, Y., Cremers, A., Emans, P., Welting, T., and Peffers, M. (2017) MicroRNA Profiling in Cartilage Ageing. *International Journal of Genomics* **2017**, 2713725
30. Chang, Z.-k., Meng, F.-g., Zhang, Z.-q., Mao, G.-p., Huang, Z.-y., Liao, W.-m., and He, A.-s. (2018) MicroRNA-193b-3p regulates matrix metalloproteinase 19 expression in interleukin-1β-induced human chondrocytes. *Journal of Cellular Biochemistry* **119**, 4775-4782
31. Díaz-Prado, S., Cicione, C., Muiños-López, E., Hermida-Gómez, T., Oreiro, N., Fernández-López, C., and Blanco, F. J. (2012) Characterization of microRNA expression profiles in normal and osteoarthritic human chondrocytes. *BMC Musculoskeletal Disorders* **13**, 144-144
32. Min, Z., zhang, R., Yao, J., Jiang, C., Guo, Y., Cong, F., Wang, W., Tian, J., Zhong, N., Sun, J., Ma, J., and Lu, S. (2015) MicroRNAs associated with osteoarthritis differently expressed in bone matrix gelatin (BMG) rat model. *International Journal of Clinical and Experimental Medicine* **8**, 1009-1017
33. Katsara, O., Attur, M., Ruoff, R., Abramson, S. B., and Kolupaeva, V. (2017) Increased activity of chondrocyte translational apparatus accompanies osteoarthritis. *Arthritis & Rheumatology (Hoboken, N.j.)* **69**, 586-597
34. Brar, G. A., and Weissman, J. S. (2015) Ribosome profiling reveals the what, when, where, and how of protein synthesis. *Nature reviews. Molecular cell biology* **16**, 651-664
35. Fields, Alexander P., Rodriguez, Edwin H., Jovanovic, M., Stern-Ginossar, N., Haas, Brian J., Mertins, P., Raychowdhury, R., Hacohen, N., Carr, Steven A., Ingolia, Nicholas T., Regev, A., and Weissman, Jonathan S. (2015) A Regression-Based Analysis of Ribosome-Profiling Data Reveals a Conserved Complexity to Mammalian Translation. *Molecular Cell* **60**, 816-827
36. Ingolia, N. T. (2016) Ribosome Footprint Profiling of Translation throughout the Genome. *Cell* **165**, 22-33
37. Zupanic, A., Meplan, C., Grellscheid, S. N., Mathers, J. C., Kirkwood, T. B. L., Hesketh, J. E., and Shanley, D. P. (2014) Detecting translational regulation by change point analysis of ribosome profiling data sets. *RNA* **20**, 1507-1518
38. Hardcastle, T. J., and Kelly, K. A. (2010) baySeq: Empirical Bayesian methods for identifying differential expression in sequence count data. *BMC Bioinformatics* **11**, 422

39. Mueller, A. J., Tew, S. R., Vasieva, O., Clegg, P. D., and Canty-Laird, E. G. (2016) A systems biology approach to defining regulatory mechanisms for cartilage and tendon cell phenotypes. *Scientific Reports* **6**, 33956
40. Santoro, A., Conde, J., Scotece, M., Abella, V., López, V., Pino, J., Gómez, R., Gómez-Reino Juan, J., and Gualillo, O. (2015) Choosing the right chondrocyte cell line: Focus on nitric oxide. *Journal of Orthopaedic Research* **33**, 1784-1788
41. Miettinen, T. P., and Björklund, M. (2015) Modified ribosome profiling reveals high abundance of ribosome protected mRNA fragments derived from 3′ untranslated regions. *Nucleic Acids Research* **43**, 1019-1034
42. Li, M., Zeringer, E., Barta, T., Schageman, J., Cheng, A., and Vlassov, A. V. (2014) Analysis of the RNA content of the exosomes derived from blood serum and urine and its potential as biomarkers. *Philosophical Transactions of the Royal Society B: Biological Sciences* **369**, 20130502
43. Valadi, H., Ekström, K., Bossios, A., Sjöstrand, M., Lee, J. J., and Lötvall, J. O. (2007) Exosome-mediated transfer of mRNAs and microRNAs is a novel mechanism of genetic exchange between cells. *Nature Cell Biology* **9**, 654
44. Zhang, Z., Harrison, P. M., Liu, Y., and Gerstein, M. (2003) Millions of Years of Evolution Preserved: A Comprehensive Catalog of the Processed Pseudogenes in the Human Genome. *Genome Research* **13**, 2541-2558
45. Tonner, P., Srinivasasainagendra, V., Zhang, S., and Zhi, D. (2012) Detecting transcription of ribosomal protein pseudogenes in diverse human tissues from RNA-seq data. *BMC Genomics* **13**, 412-412
46. Lilly, M., Sandholm, J., Cooper, J. J., Koskinen, P. J., and Kraft, A. (1999) The PIM-1 serine kinase prolongs survival and inhibits apoptosis-related mitochondrial dysfunction in part through a bcl-2-dependent pathway. *Oncogene* **18**, 4022
47. Friedlander, R., Gagliardini, V., Rotello, R., and Yuan, J. (1996) Functional role of interleukin 1 beta (IL-1 beta) in IL-1 beta- converting enzyme-mediated apoptosis. *The Journal of Experimental Medicine* **184**, 717-724
48. Kasza, A., Wyrzykowska, P., Horwacik, I., Tymoszuk, P., Mizgalska, D., Palmer, K., Rokita, H., Sharrocks, A. D., and Jura, J. (2010) Transcription factors Elk-1 and SRF are engaged in IL1-dependent regulation of ZC3H12A expression. *BMC Molecular Biology* **11**, 14
49. Andreev, D. E., O'Connor, P. B. F., Fahey, C., Kenny, E. M., I.M., T., Dmitriev, S. E., Cormican, P., Morris, D. W., Shatsky, I. N., and Baranov, P. V. (2015) Translation of 5′ leaders is pervasive in genes resistant to eIF2 repression *eLIFE* **4**
50. Zou, K., Ouyang, Q., Liao, H., and Zheng, J. (2017) A global characterization of the translational and transcriptional programs induced by methionine restriction through ribosome profiling and RNA-seq. *BMC Genomics.* **18**
51. Scanzello, C. R., and Goldring, S. T. (2012) The Role of Synovitis in Osteoarthritis pathogenesis. *Bone* **51**, 249-257
52. Mengshol, J. A., Vincenti, M. P., and Brinckerhoff, C. E. (2001) IL-1 induces collagenase-3 (MMP-13) promoter activity in stably transfected chondrocytic cells: requirement for Runx-2 and activation by p38 MAPK and JNK pathways. *Nucleic Acids Research* **29**, 4361-4372
53. Henrotin, Y., Kurz, B., and Aigner, T. (2005) Oxygen and reactive oxygen species in cartilage degradation: friends or foes? *Osteoarthritis and Cartilage* **13**, 643-654
54. Lepetsos, P., and Papavassiliou, A. G. (2016) ROS/oxidative stress signaling in osteoarthritis. *Biochimica et Biophysica Acta (BBA) - Molecular Basis of Disease* **1862**, 576-591
55. Kabe, Y., Ando, K., Hirao, S., Yoshida, M., and Handa, H. (2005) Redox Regulation of NF-κB Activation: Distinct Redox Regulation Between the Cytoplasm and the Nucleus. *Antioxidants & Redox Signaling* **7**, 395-403
56. Lane, R. S., Fu, Y., Matsuzaki, S., Kinter, M., Humphries, K. M., and Griffin, T. M. (2015) Mitochondrial respiration and redox coupling in articular chondrocytes. *Arthritis Research & Therapy* **17**, 54
57. Mathy-Hartert, M., Hogge, L., Sanchez, C., Deby-Dupont, G., Crielaard, J. M., and Henrotin, Y. (2008) Interleukin-1β and interleukin-6 disturb the antioxidant enzyme system in bovine

chondrocytes: a possible explanation for oxidative stress generation. *Osteoarthritis and Cartilage* **16**, 756-763
58. Katsara, O., Attur, M., Ruoff, R., Abramson, S. B., and Kolupaeva, V. (2017) Increased Activity of the Chondrocyte Translational Apparatus Accompanies Osteoarthritic Changes in Human and Rodent Knee Cartilage. *Arthritis & rheumatology* **69**, 586-597
59. Katsara, O., and Kolupaeva, V. (2018) mTOR-mediated inactivation of 4E-BP1, an inhibitor of translation, precedes cartilage degeneration in rat osteoarthritic knees. *J Orthop Res* **36**, 2728-2735
60. Balaskas, P., Goljanek-Whysall, K., Clegg, P., Fang, Y., Cremers, A., Emans, P., Welting, T., and Peffers, M. (2017) MicroRNA Profiling in Cartilage Ageing. *International journal of genomics* **2017**, 2713725
61. Steinbusch, M. M., Fang, Y., Milner, P. I., Clegg, P. D., Young, D. A., Welting, T. J., and Peffers, M. J. (2017) Serum snoRNAs as biomarkers for joint ageing and post traumatic osteoarthritis. *Sci Rep* **7**, 43558
62. Ashraf Kharaz, Y., Zamboulis, D., Sanders, K., Comerford, E., Clegg, P., and Peffers, M. (2017) Comparison between chaotropic and detergent-based sample preparation workflow in tendon for mass spectrometry analysis. *PROTEOMICS* **17**, 1700018
63. Peffers, M. J., Thorpe, C. T., Collins, J. A., Eong, R., Wei, T. K. J., Screen, H. R. C., and Clegg, P. D. (2014) Proteomic Analysis Reveals Age-related Changes in Tendon Matrix Composition, with Age- and Injury-specific Matrix Fragmentation. *Journal of Biological Chemistry* **289**, 25867-25878
64. Ingolia, N. T., Brar, G. A., Rouskin, S., McGeachy, A. M., and Weissman, J. S. (2012) The ribosome profiling strategy for monitoring translation in vivo by deep sequencing of ribosome-protected mRNA fragments. *Nature Protocols* **7**, 1534
65. Michel, A. M., Mullan, J. P. A., Velayudhan, V., O'Connor, P. B. F., Donohue, C. A., and Baranov, P. V. (2016) RiboGalaxy: A browser based platform for the alignment, analysis and visualization of ribosome profiling data. *RNA Biology* **13**, 316-319

**FOOTNOTES**

Funding was provided by the BBSRC, the University of Liverpool's Department of Musculoskeletal Biology and the University of Liverpool Technology Directorate.

The abbreviations used are: 3'UTR, 3' untranslated region; CCL, chemokine (C-C motif) ligand; CDS, coding sequence; DAVID, database for annotation, visualisation and integrated discovery; ER, endoplasmic reticulum; ECM, extracellular matrix; GOterm_BP, gene ontology term_biological processes; HAC, human articular chondrocytes; IL-1, interleukin-1; KEGG, Kyoto encyclopaedia of genes and genomes; MMP, matrix metalloproteinase; OA, osteoarthritis; ORF, open reading frame; RPFs, ribosome protected fragments; SOD, superoxide dismutase; STRING, search took for the retrieval of interacting genes/proteins; TNFα, tumour necrosis factor alpha; TNFAIP, TNFα induced protein.

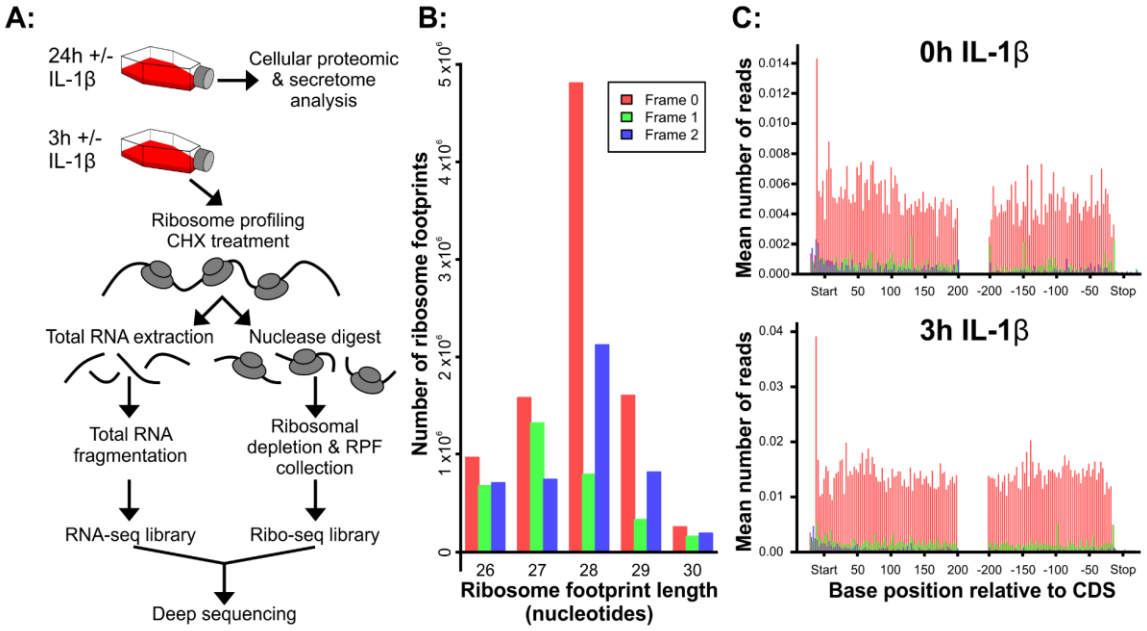


Fig. 1

**Figure 1. Ribosome profiling workflow and sequencing data. A**) SW1353 workflow: cells were treated, for 3 or 24 hours with or without IL-1β. Media was harvested for secretome proteomic analysis and cells were harvested for intracellular proteomic analysis after 24h IL-1β exposure. Ribosome profiling was performed on cells exposed to IL-1β for 0h and 3h. **B**) To obtain triplet periodicity of ribosome protected fragments, sequencing results (FASTQ files) from amplified libraries were first uploaded to RiboGalaxy. The 5'-AGATCGGAAGAGCACACGTCT-3' adapter sequence and rRNA sequences were removed using Cutadapt and Bowtie. Sequences were then aligned to the human transcriptome (GRCh38/hg38) using Bowtie prior to riboSeqR analysis. From the riboSeqR analysis, triplet periodicity showed that most sequencing reads were 28 nucleotides in length and in frame 1 (red). **C**) RiboGalaxy was next used to perform a metagene analysis of the ribosome density and showed similar ribosomal coverage over all transcripts that are 28 nucleotides in length. This representative metagene analysis reflects triplet periodicity results in that the majority of 28mer transcripts are in frame 1 (red).

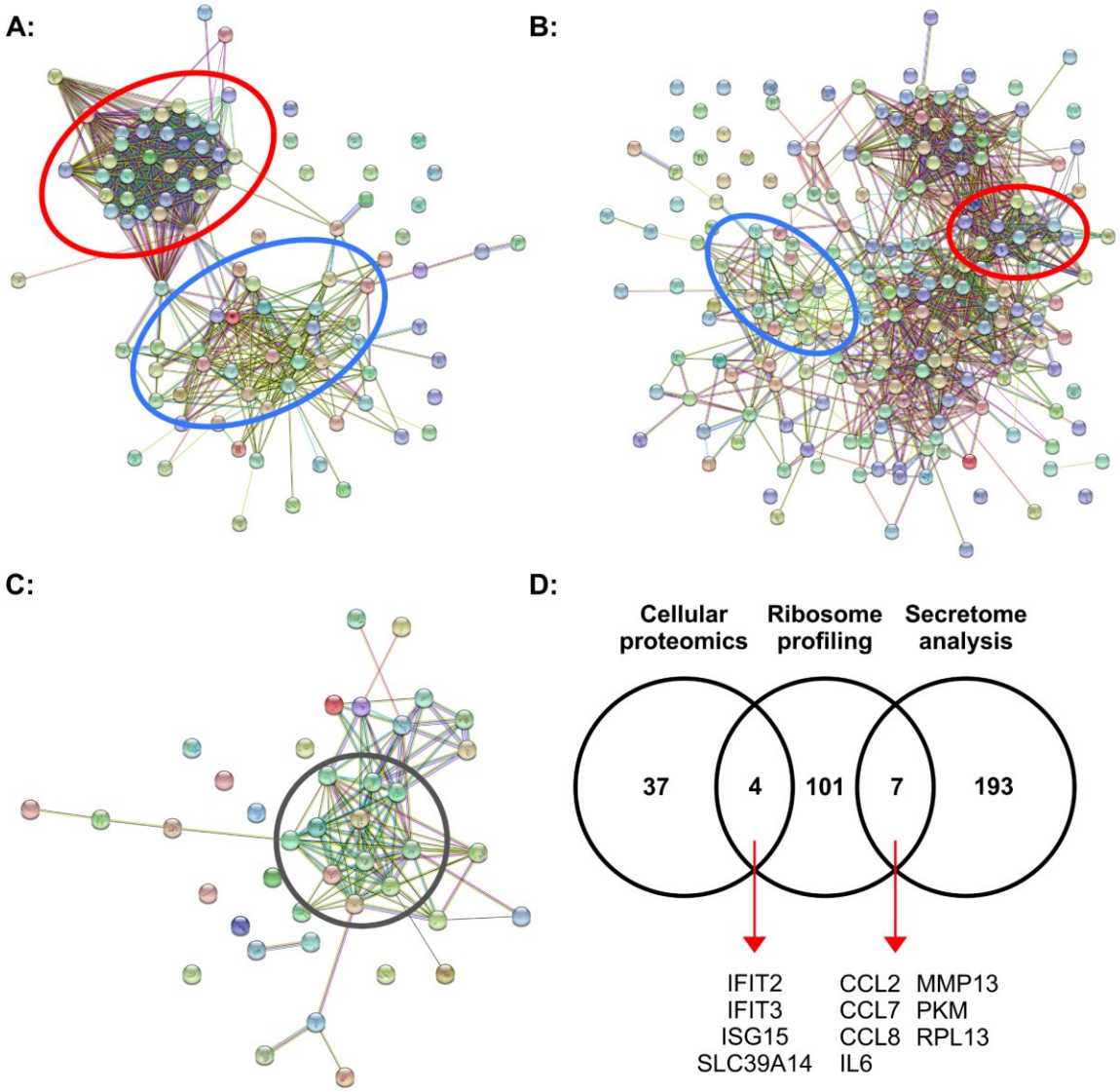


Fig. 2

**Figure 2. SW1353 transcript/proteomic analyses. A**) STRING analysis of the 112 transcripts statistically significant differentially translated RPFs from the 3h +/- IL-1β treatment. **B**) STRING analysis of the 200 statistically significant differentially secreted proteins from the 24h +/- IL-1β treatment and **C**) the 41 statistically significant differentially expressed proteins identified in the cell layer proteomic analysis. **D**) Venn diagram showing the relationship of the top 200 transcripts/proteins identified through cellular proteomic analysis, ribosome profiling and secretome analysis. Red circles highlight clustering of ribosomal-associated transcripts/proteins and blue circles highlight clustering of inflammatory-associated transcripts/proteins. Grey circle highlights interferon-associated proteins. A full list of transcripts/proteins and the STRING networks with labels can be found in supplementary data tables.

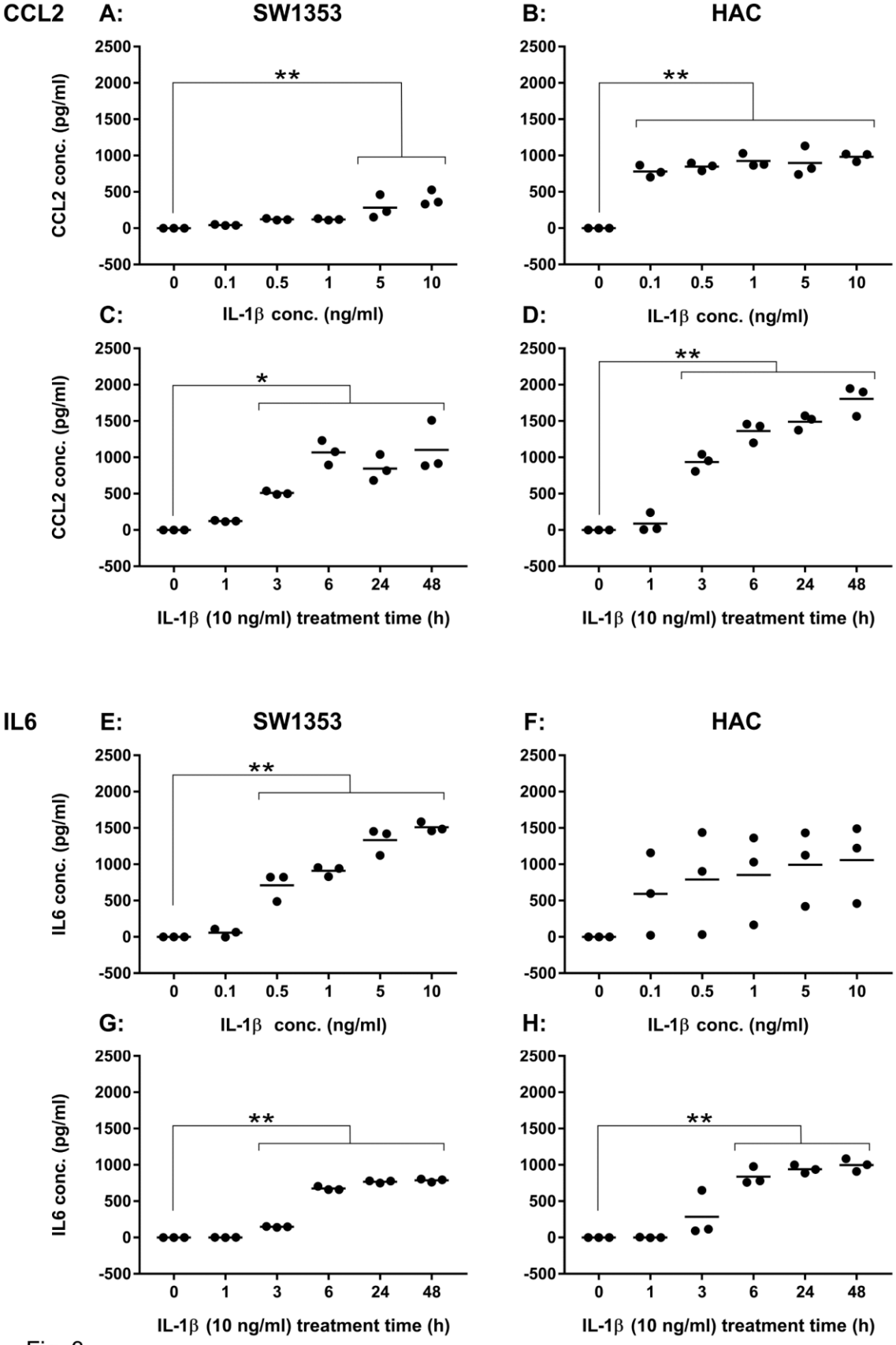
CCL2
A:
SW1353
B:
HAC
CCL2 conc. (pg/ml)
2500
2000
1500
1000
500
0
-500
**
0
0.1
0.5
1
5
10
IL-1β conc. (ng/ml)
C:
D:
*
**
0
1
3
6
24
48
IL-1β (10 ng/ml) treatment time (h)
IL6
E:
F:
IL6 conc. (pg/ml)
G:
H:

Fig. 3

**Figure 3. Cytokine secretion levels following exposure to IL-1β. A**) CCL2 levels in SW1353 medium following 24 hour exposure to IL-1β at concentrations ranging from 0 to 10 ng/ml. **B**) CCL2 levels in HAC (M70, M76, M86) medium following 24 hour exposure to IL-1β at concentrations ranging from 0 to 10 ng/ml. **C**) CCL2 levels in SW1353 medium following 10 ng/ml IL-1β treatment for 0 to 48 hours. **D**) CCL2 levels in HAC (M69, F80, F86) medium following 10 ng/ml IL-1β treatment for 0 to 48 hours. **E**) IL-6 levels in SW1353 medium following 24 hour exposure to IL-1β at concentrations ranging from 0 to 10 ng/ml. **F**) IL-6 levels in HAC (M70, M76, M86) medium following 24 hour exposure to IL-1β at concentrations ranging from 0 to 10 ng/ml. **G**) IL-6 levels in SW1353 medium following 10 ng/ml IL-1β treatment for 0 to 48 hours. **H**) IL-6 levels in HAC (M69, F80, F86) medium following 10 ng/ml IL-1β treatment for 0 to 48 hours. Data was considered significant if $p=<0.05$ (*) and $p=<0.01$ (**) following Dunnett's multiple comparison tests.

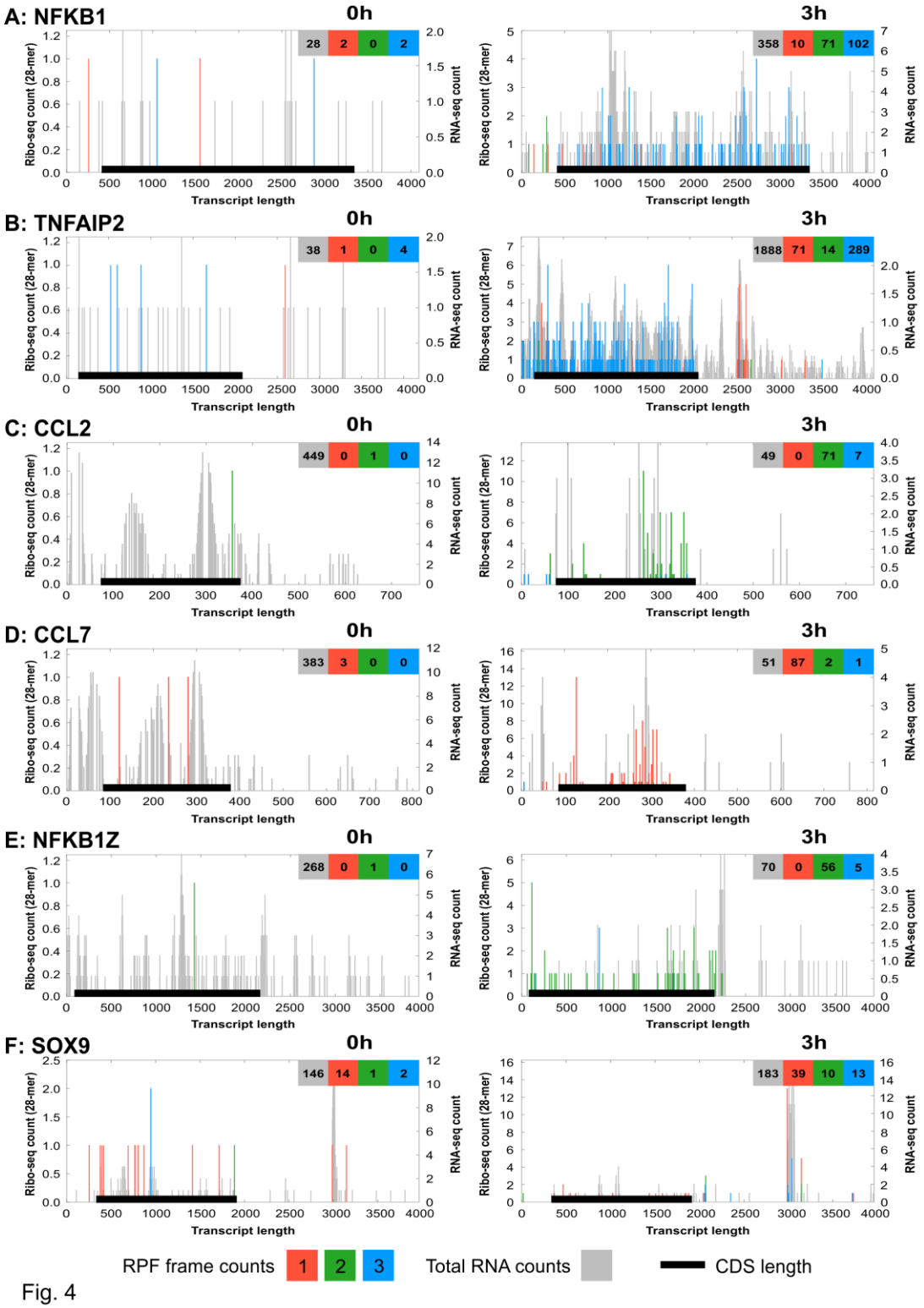


Fig. 4

**Figure 4. Riboplots of differentially translated mRNA transcripts.** Using the Ribo-Seq alignment files generated from aligning the sequencing data to the human transcriptome, riboplots were generated using the RiboPlot suite on RiboGalaxy for transcripts that were differentially translated between 0h and 3h IL-1β exposure. Riboplots show the sub-codon ribosome footprint and the open reading frame organisation for both the 0h and 3h time points for **A**) NFKB1 (NM_003998.3), **B**) TNFAIP2

(NM_006291), **C**) CCL2 (NM_002982.3), **D**) CCL7 (NM_006273.3), **E**) NFKB1Z (NM_031419.3) and **F**) SOX9 (NM_000346.3). Ribo-counts shown for frame 1 (red), Frame 2 (green) and frame 3 (blue). Total RNA reads in the background (grey) represent the total mRNA for all frames of the respective transcript. The black lines represent the CDS position within the transcript. X-axis represents transcript length (in nucleotides) 5' to 3'. Left y-axis represents the ribo-seq counts for all three reading frames (RPFs). Right y-axis represents the RNA-seq counts for total RNA.

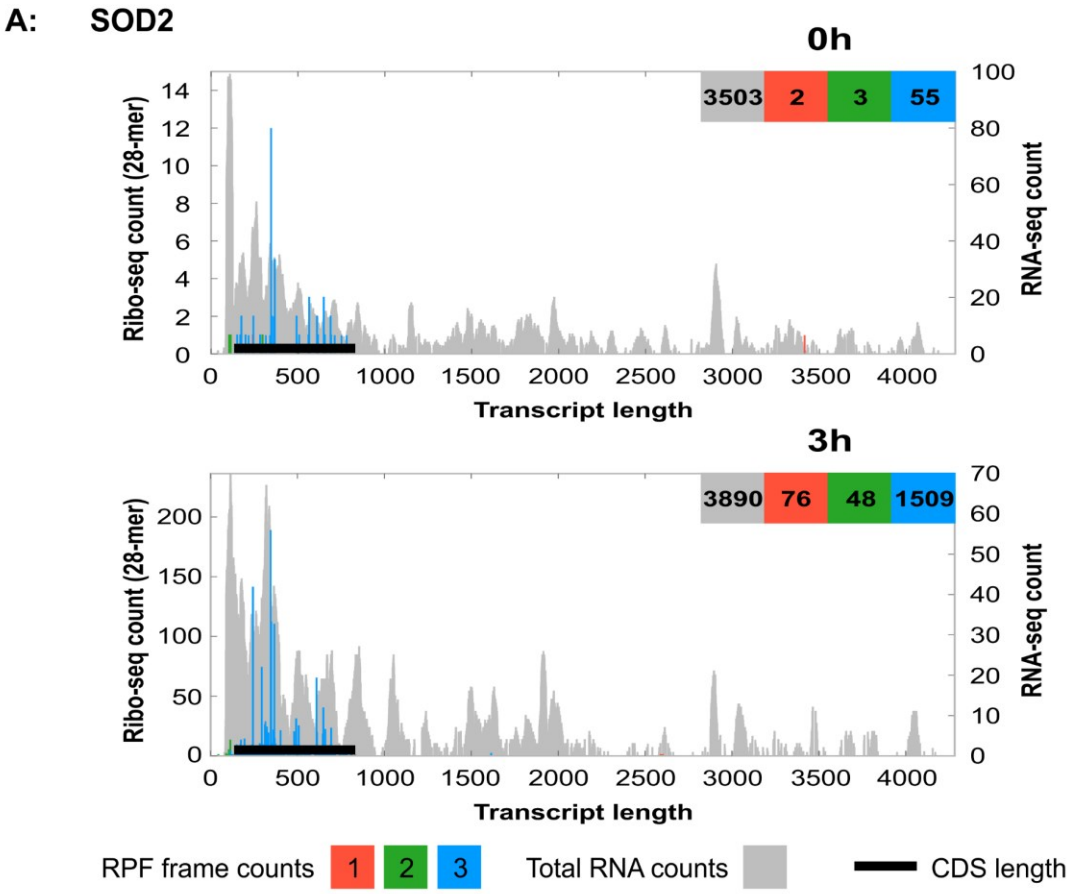
A:
SOD2
0h
3503
2
3
55
Ribo-seq count (28-mer)
RNA-seq count
Transcript length
3h
3890
76
48
1509
RPF frame counts
Total RNA counts
CDS length
B:
kDa
0 1 3 6 24 48 hours
0 0.1 0.5 1 5 10 ng/ml
C:
ROS activity normalised to positive control
IL-1β (10ng/ml) treatment time (h)
IL-1β conc. (ng/ml)

Fig. 5

**Figure 5. IL-1β treatment causes an increase in SOD2 mRNA and protein expression in SW1353 cells. A**) Riboplot for SOD2 (NM_000636.3). Ribo-counts shown for frame 1 (red), Frame 2 (green) and frame 3 (blue). Total RNA reads in the background (grey) represent the total mRNA for all frames of the respective transcript. The black lines represent the CDS position within the transcript. X-axis represents transcript length (in nucleotides). Left y-axis represents the ribo-seq counts for all three reading frames. Right y-axis represents the RNA-seq counts for total RNA. **B**) Western blotting for SOD2 (22 kDa) in SW1353 intracellular protein lysates treated with 10 ng/ml IL-1β for 0 to 48 hours (left-top) and corresponding total protein stain (left-bottom), plus western blotting for SOD2 in SW1353 intracellular protein lysates treated with 0 to 10 ng/ml IL-1β for 24 hours (right-top) and corresponding total protein stain (right-bottom). **C**) CM-$H_2$DCFDA assay for SW1353 treated with 10 ng/ml IL-1β for 0 to 48 hours (left) and treated with 0 to 10 ng/ml IL-1β for 24 hours (right). Data variance determined by ANOVA $p<0.05$ (†) or $p<0.01$ (††). * Significant difference vs. 0 hour treatment time following Dunnett's multiple comparison testing ($p<0.05$).